Molecular Therapy
Oncolytics
Original Article

Non-glycanated Decorin Is a Drug Target on Human Adipose Stromal Cells

Alexes C. Daquinag,[1] Ali Dadbin,[1] Brad Snyder,[2] Xiaoping Wang,[3,4,5] Aysegul A. Sahin,[6] Naoto T. Ueno,[3,4,5] and Mikhail G. Kolonin[1]

[1]The Brown Foundation Institute of Molecular Medicine, University of Texas Health Science Center at Houston, Houston, TX 77030, USA; [2]Department of Surgery, University of Texas Health Science Center at Houston, Houston, TX 77030, USA; [3]Department of Breast Medical Oncology, The University of Texas MD Anderson Cancer Center, Houston, TX 77030, USA; [4]Morgan Welch Inflammatory Breast Cancer Research Program and Clinic, The University of Texas MD Anderson Cancer Center, Houston, TX 77030, USA; [5]Section of Translational Breast Cancer Research, The University of Texas MD Anderson Cancer Center, Houston, TX 77030, USA; [6]Department of Pathology, The University of Texas MD Anderson Cancer Center, Houston, TX 77030, USA

Adipose stromal cells (ASCs) have been identified as a mesenchymal cell population recruited from white adipose tissue (WAT) by tumors and supporting cancer progression. We have previously reported the existence of a non-glycanated decorin isoform (ngDCN) marking mouse ASCs. We identified a peptide CSWKYWFGEC that binds to ngDCN and hence can serve as a vehicle for ASC-directed therapy delivery. We used hunter-killer peptides composed of CSWKYWFGEC and a pro-apoptotic moiety to deplete ASCs and suppress growth of mouse tumors. Here, we report the discovery of the human non-glycanated decorin isoform. We show that CSWKYWFGEC can be used as a probe to identify ASCs in human WAT and tumors. We demonstrate that human ngDCN is expressed on ASC surface. Finally, we validate ngDCN as a molecular target for pharmacological depletion of human ASCs with hunter-killer peptides. We propose that ngDCN-targeting agents could be developed for obesity and cancer treatment.

INTRODUCTION

There is an urgent need to identify novel anti-cancer druggable targets and therapies. Our previous studies have elucidated the role of tumor stromal cells derived from white adipose tissue (WAT), which contains large numbers of adipose stromal cells (ASCs), the mesenchymal stromal cell (MSC) population expanded in obesity.[1–5] We have shown that WAT contributes to the pool of tumor stromal cells[6,7] in both mice[5] and patients.[8,9] There is accumulating evidence that WAT surrounding the tumor is a key source of tumor stroma and that adenocarcinoma growth and progression is associated with infiltration of ASCs derived from WAT. Our recent study has identified ASCs recruitment by tumors as the mechanism through which WAT promotes cancer progression and link ASCs recruitment with poor patient survival.[2] In animal studies, administered ASCs engraft tumors, which results in accelerated cancer progression.[3–5] Our findings confirmed by data from other groups[10–14] demonstrate tumor recruitment of endogenous ASCs and indicate that ASCs promote survival and proliferation of neighboring malignant cells. The apparent contribution of ASCs to the tumor microenvironment has raised a question regarding the safety of lipotransfer procedures in cancer patients.[15–17] There is also emerging evidence that ASCs contribute to therapy resistance of various cancers.[18,19]

We and others have discovered that ASCs can be identified as cells positive for mesenchymal markers and CD34 while negative for endothelial (CD31) and hematopoietic (CD45) markers.[20,21] We had originally reported platelet-derived growth factor receptor-alpha (PDGFRα) and PDGFR-beta (PDGFRβ), also known as CD140a and CD140b, as mesenchymal markers expressed on human ASCs.[21] Subsequently, PDGFRα and PDGFRβ have been validated as adipocyte progenitors in mice by lineage tracing.[22–24] We have shown that stromal cells expressing either PDGFRα or PDGFRβ are recruited by tumors in mouse models.[25] However, both PDGFRα and PDGFRβ, as well as other mesenchymal markers, are expressed on various cell populations in different organs. Therefore, they cannot serve as specific markers of ASCs, and the lack of molecules expressed on ASCs, but not on other MSCs, has impeded the progress in the field. We previously reported that ΔDCN, a truncated isoform of matricellular proteoglycan decorin (DCN), is expressed on the surface of mouse ASCs.[26] This isoform lacks the N-terminal segment and is free of the glycosaminoglycan chain. A cyclic peptide with the sequence CSWKYWFGEC (termed WAT7) isolated from a combinatorial peptide library based on its ASC homing was shown to bind ΔDCN.[26] Whereas full-length DCN, expressed in many organs, is exported extracellularly to crosslink collagen, the non-glycanated isoform, ΔDCN, is generated in WAT and is exposed on ASC surface. We showed that CSWKYWFGEC is specific for ASCs and does not recognize MSCs in other organs.[26]

Based on the ability of CSWKYWFGEC to undergo ASC internalization,[26] by analogy with our previous studies,[27] we designed a bimodal peptide D-WAT composed of CSWKYWFGEC and of the

Received 27 January 2017; accepted 10 May 2017;
http://dx.doi.org/10.1016/j.omto.2017.05.003.

Correspondence: Mikhail G. Kolonin, The Brown Foundation Institute of Molecular Medicine, University of Texas Health Science Center at Houston, 1825 Pressler Street, Room 630-G, Houston, TX 77030, USA.
E-mail: mikhail.g.kolonin@uth.tmc.edu

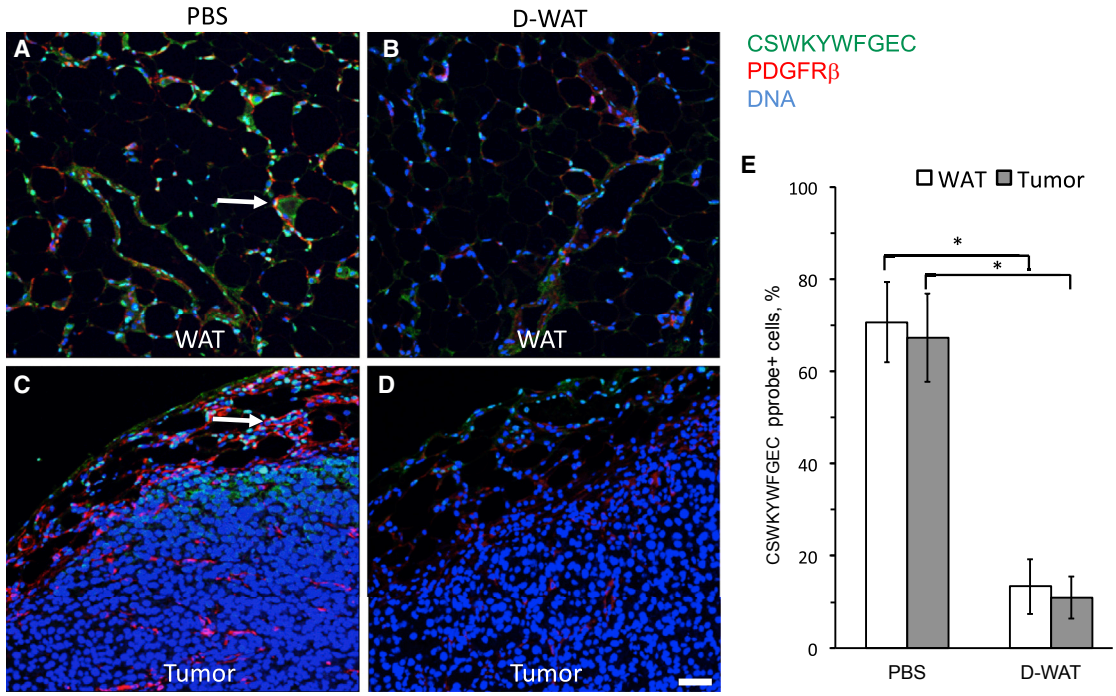

Figure 1. CSWKYWFGEC Peptide Probe Identifies ASC in Mouse WAT and Tumors

Prostate adenocarcinoma RM1 allografts grown in immunocompetent mice treated with PBS (A and C) or ASC-targeting peptide D-WAT (B and D). WAT (A and B) and tumor (C and D) sections were incubated with biotinylated ASC-binding peptide CSWKYWFGEC and then subjected to immunofluorescence with antibodies specific for mouse PDGFRβ (red) to localize ASCs and with streptavidin (green) to localize the CSWKYWFGEC peptide. Note CSWKYWFGEC signal on PDGFRβ-expressing ASCs in control WAT and tumors is shown (arrows). Nuclei are blue. The scale bar represents 50 μm. (E) Quantification of data from (A)–(D) shows that the frequency of CSWKYWFGEC-bound cells in WAT and tumor capsule is reduced upon D-WAT peptide treatment. Plotted are mean ± SEM for multiple fields (n = 10). *$p < 0.01$ (Student's t test). Experiments were performed twice with similar results.

KLAKLAKKLAKLAK domain linked via aminohexanoic acid. To circumvent the problem of short half-life of peptides in vivo due to proteolytic degradation, D-WAT is synthesized with all amino acids as D-enantiomers, which are not recognized by proteases and the immune system.[28] D-WAT has a dose-dependent and specific cytotoxicity toward ASCs adherent in culture, whereas other cell types were not affected.[25,29] In vivo, using flow cytometry and immunofluorescence (IF), we demonstrated depletion of ASCs, but not of MSCs, in other organs. In the mouse model, ASC depletion expectedly resulted in WAT growth suppression and adipose tissue browning.[29] Recently, we reported that targeting ASCs via ΔDCN also suppresses tumor growth.[25] In that report, we demonstrated that D-WAT treatment specifically depletes tumor stromal and perivascular cells without directly killing malignant cells or tumor-infiltrating leukocytes. ASC cytoablation reduced tumor vascularity and cell proliferation, hence causing hemorrhaging, necrosis, and tumor growth suppression in several mouse carcinoma models. We also validated a D-WAT derivative with a pro-apoptotic domain $KFAKFAK_2$ that had higher cytoablative activity.

Whereas our previous studies have demonstrated that ASCs can serve as a drug target in mouse models, the clinical relevance of the discovery of CSWKYWFGEC peptide and ΔDCN has been unclear. Because DCN is evolutionary conserved,[26] we investigated whether there is a human isoform serving as an ASC marker. Here, we present data revealing the expression of non-glycanated (ngDCN) fragment of human DCN, an equivalent of ΔDCN, on both subcutaneous (s.c.) and intraperitoneal (i.p.) visceral ASCs. We show that CSWKYWFGEC can be used as a probe to identify ASCs not only in mouse but also in human WAT and tumors. Finally, we show that human ngDCN is also targeted by CSWKYWFGEC-directed hunter-killer peptides, thus enabling depletion of human $PDGFR\beta^+$ ASCs.

RESULTS

Peptide CSWKYWFGEC as a Probe to Identify ASCs in Tissue Sections

To investigate whether a DCN isoform recognized by CSWKYWFGEC exists in humans, we tested whether this peptide can serve as a probe similar to an antibody. As a proof of principle, we tested this approach to identify ASCs in mouse paraffin tissue sections using CSWKYWFGEC peptide. Deparaffinized sections were incubated with biotinylated CSWKYWFGEC and subsequently with a streptavidin-fluorophore conjugate. As shown in Figure 1A, the peptide bound to PDGFRβ-expressing cells in WAT, as expected. Importantly, by incubating the peptide with sections of RM1 adenocarcinoma tumors grown in mice, we demonstrated that it binds to a

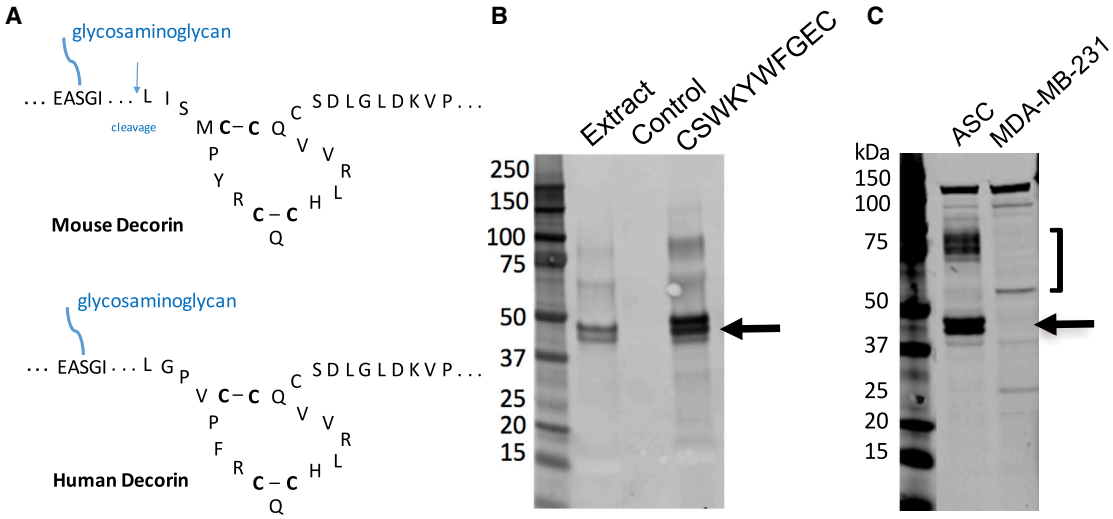

Figure 2. Human ASCs Express Non-glycanated DCN that Binds to CSWKYWFGEC

(A) A fragment of mouse and human DCN showing disulfide bonds and the cleavage site in mouse DCN. N-terminal and C-terminal sequences, as well as sequence downstream of GAG attachment site, are abbreviated (...). (B) Membrane proteins extracted from s.c. ASCs of a bariatric surgery patient 1 were incubated with CSWKYWFGEC-conjugated beads or control deactivated unconjugated beads. After washing, eluted proteins were subjected to immunoblotting with anti-human decorin antibodies. (C) Proteins extracted from s.c. ASCs of a bariatric surgery patient 2 and human breast adenocarcinoma cells (MDA-MB-231) were subjected to immunoblotting with anti-human decorin antibodies. Arrow points to the band doublet, where the upper band is the core decorin.] indicates glycanated decorin. Experiments were performed for i.p. and s.c. WAT of three patients with similar results.

sub-population of cells in tumor stroma (Figure 1C). This indicates that some of the tumor-recruited ASCs may serve as a direct target of CSWKYWFGEC-directed hunter-killer peptides. To validate peptide specificity, we incubated it with tissues from mice treated with an ASC-targeted hunter-killer peptide WAT7-KFAKFAK$_2$ (here termed D-CAN), which we reported previously.[25] As expected, the frequency of cells bound with CSWKYWFGEC and expressing PDGFRβ was dramatically reduced after D-WAT treatment (Figures 1B–1E). This indicates that peptide CSWKYWFGEC specifically identifies ΔDCN-expressing cells in IF applications.

Human ASCs Express Non-glycanated DCN Recognized by CSWKYWFGEC

Comparison of mouse and human DCN amino termini revealed the high ortholog similarity. Specifically, the positions of cysteines forming disulfide bonds downstream of the glycanation site and the site of mouse DCN cleavage resulting in ΔDCN showing disulfide bonds and the cleavage site in mouse DCN were conserved (Figure 2A). Based on that, we predicted that cleavage of human DCN may take place. To test this directly, we extracted proteins from ASCs derived from s.c. and i.p. WAT of three bariatric surgery patients. Membrane proteins were incubated with CSWKYWFGEC-conjugated beads or deactivated unloaded beads as a negative control. After washing, eluted proteins were subjected to immunoblotting with anti-human decorin antibodies. This revealed the presence of the core DCN band and a smaller band corresponding in size to ΔDCN specifically pulled down with CSWKYWFGEC (Figure 2B). Expression of the two DCN isoforms was confirmed for both s.c. and i.p. of different patients analyzed (Figure S1A). We also performed immunoblotting with anti-human DCN antibodies directly on ASC extracts. Each of the two ngDCN forms was more abundant than glycanated DCN (Figure 2C). Human breast cancer cell line MDA-MB-231 used as a negative control was analyzed in parallel. There was no non-glycanated DCN bands observed in proteins extracted from MDA-MB-231 cells (Figure 2C). Non-glycanated DCN was also undetectable in other human cell lines, including PC3 and DU145 prostate adenocarcinoma, HepG2 liver adenocarcinoma, and HEK293 embryonic kidney cells (Figures S1A and S1B). This indicates that, like in mice, human ngDCN is selectively expressed by ASCs.

CSWKYWFGEC Peptide as a Probe Binding Human ASCs

We then tested whether peptide CSWKYWFGEC can specifically identify mouse and human ngDCN in IF applications. First, we demonstrated peptide binding specificity by comparing wild-type (WT) and DCN-null mouse embryonic fibroblasts (MEFs).[30] Cells growing in culture were incubated with biotinylated CSWKYWFGEC and then with streptavidin-Cy3 conjugate. Upon washing, notably higher binding of CSWKYWFGEC to WT MEFs was observed, whereas a control peptide CWLGEWLGC mimicking the β1 integrin-interacting protein SPARC[31] displayed no selectivity (Figure S1C). We then compared peptide binding to human ASCs and PC3 prostate adenocarcinoma cells used as a negative control. CSWKYWFGEC bound to the surface of ASC, whereas signal on PC3 cells was very low (Figure 3A). We preformed the same experiment with a scrambled peptide CWWGSFYEKC and an unrelated brown fat-homing peptide (BAT8) reported previously.[32] The two biotinylated control peptides did not bind to human ASCs (Figure 3A), confirming that

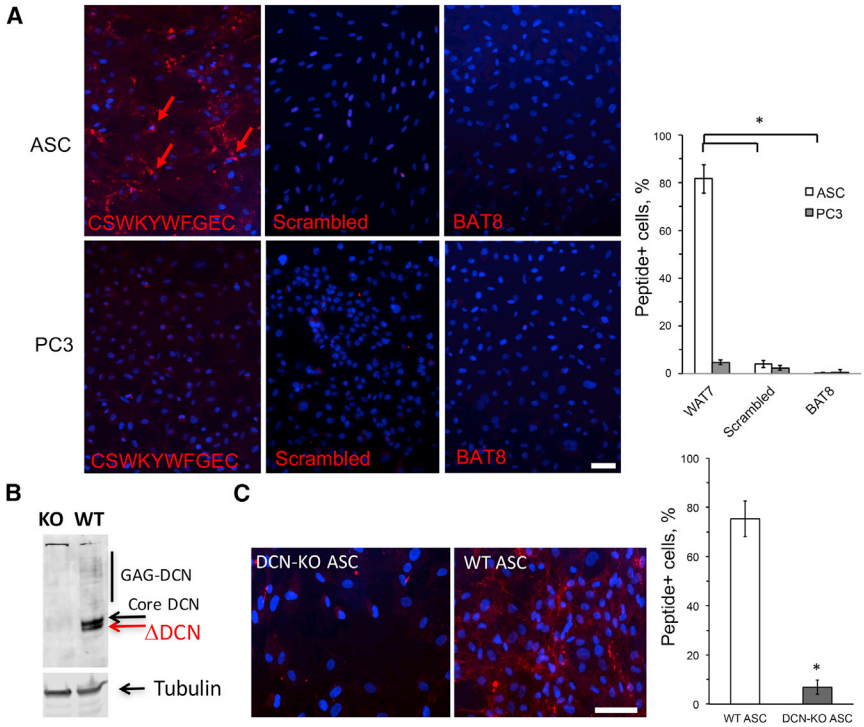

Figure 3. CSWKYWFGEC Binds to ngDCN on Human ASC Surface

(A) Live human ASCs from s.c. WAT of a bariatric surgery patient 1 and prostate adenocarcinoma cells (PC3) cells were incubated with 20 nM biotinylated CSWKYWFGEC, a scrambled peptide CWWGSFYEKC, or a control biotinylated peptide (BAT8). After incubation in 10% FBS/DMEM media for 2 hr, washing, and fixation, cells were incubated with streptavidin-Cy3 and stained with DAPI. Plotted are mean ± SEM for multiple fields (n = 10). *p < 0.01 (Student's t test). (B) Anti-DCN immunoblotting on protein extracts from human ASCs in which DCN was deleted (KO) and wild-type parental ASCs (WT) used as control. β- tubulin, loading control. (C) Live human DCN null and control ASCs were incubated with 20 nM biotinylated CSWKYWFGEC. After incubation in 10% FBS/DMEM media for 2 hr, washing, and fixation, cells were incubated with streptavidin-Cy3 and stained with DAPI. Nuclei are blue. The scale bar represents 50 μm. Plotted are mean ± SEM for multiple fields (n = 10). *p < 0.01 (Student's t test). Experiments were performed for i.p. and s.c. WAT of three patients with similar results.

CSWKYWFGEC binding is specific. We also generated DCN-null human ASCs using the CRISPR/Cas9 approach to demonstrate that CSWKYWFGEC binding is contingent on DCN expression (Figure 3B). Indeed, biotinylated CSWKYWFGEC bound to unmodified ASCs, whereas the signal on DCN-knockout (KO) ASCs was dramatically reduced (Figure 3C). Furthermore, we used CSWKYWFGEC peptide as a probe on paraffin sections of human tissues. An array of human organs was analyzed. Strikingly, CSWKYWFGEC showed binding to stromal cells in both s.c. WAT (Figure 4A) and periprostatic i.p. WAT (Figure S2A), whereas the scrambled peptide (Figure 4B) or a control peptide BAT8 (Figure S2B) did not bind to cells of WAT. Importantly, CSWKYWFGEC displayed no binding to cells of lung (Figure 4C) or other control organs, including spleen, heart, skeletal muscle, pancreas, kidney, liver, and brain (Figure S2A). We also analyzed peptide binding to human breast cancer tissues. CSWKYWFGEC bound to stroma in WAT surrounding the tumor as well as to tumor stromal cells (Figure 4D). CSWKYWFGEC binding to tumor stromal cells was observed for different cancer subtypes and grades (Figure S3).

Human ASC Targeting with a Hunter-Killer Peptide

Next, we tested whether ngDCN-homing hunter killer peptides could be used for human ASC ablation. We incubated human ASCs and control cells with increasing concentrations of peptide D-CAN that has been shown to kill mouse ASCs.[25] Trypan blue exclusion assay was used to assess cell death. At the concentration of 0.05 mM, previously reported effective for mouse ASC,[25,29] D-CAN also killed ~50% of human ASCs (Figure 5A). Importantly, control human cell lines were not killed by D-CAN at the concentration lethal for ASCs (Figure 5A). Both subcutaneous and visceral ASCs from three different patients were confirmed to be sensitive to D-CAN treatment (Figure S4A). Untargeted pro-apoptotic domain did not cause cell death at that concentration and killed cells only nonspecifically starting at 1 mM (Figure S4B). Importantly, by using human DCN-null ASCs (Figure 3B), we showed that D-CAN kills only cells that express DCN (Figure 5B). Finally, we tested whether CSWKYWFGEC peptide kills a sub-population of human ASCs with a selectivity reported in mice.[25,29] By analyzing sections derived from bariatric surgery patients, we discovered that human WAT contains PDGFRα$^+$ PDGFRβ$^-$ ASCs in the stroma and PDGFRα$^-$PDGFRβ$^+$ ASCs in close association with the blood vessel lumen (Figure 6A). Thus, human WAT has two sub-populations of ASCs that we previously reported in mice.[29] Like in mice, D-WAT peptide killed some, but not all, human ASCs in cell culture, as revealed by trypan blue staining (Figure 6B). To identify the sensitive ASC sub-population, we performed IF with PDGFRα and PDGFRβ antibodies while also immuno-detecting cleaved caspase 3 (a marker of apoptosis). Colocalization studies clearly showed that D-WAT induced apoptosis of PDGFRβ$^+$, but not of PDGFRα$^+$, ASCs. We conclude that, like in mice, ngDCN is selectively expressed on PDGFRα$^-$PDGFRβ$^+$ ASCs that can be targeted with CSWKYWFGEC-directed hunter killer peptides.

DISCUSSION

New molecular therapeutics are awaited to effectively suppress cancer aggressiveness and progression to metastatic stage. Inability of available drugs to overcome the resistance of cancer to treatment indicates the existence of untargeted cell populations driving the disease. Growth and metastasis of solid tumors relies on the tumor stroma, the infiltrating non-malignant fibroblastoid cells.[1,33] Disease

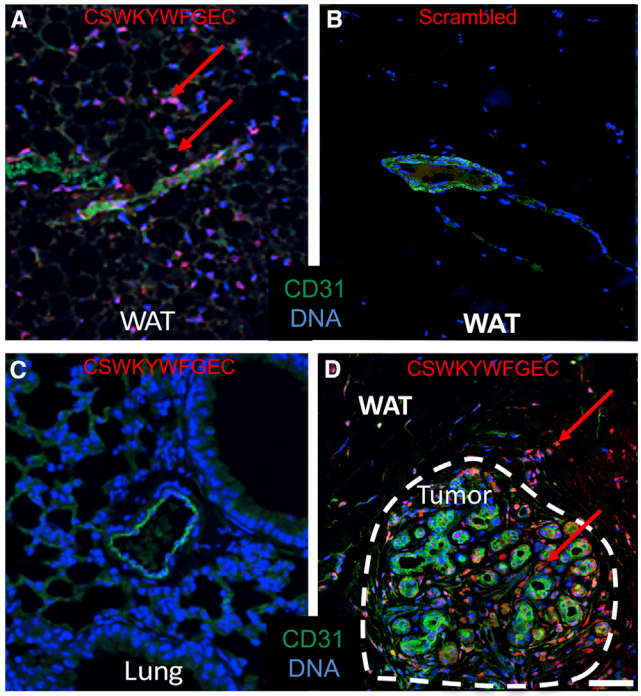

Figure 4. CSWKYWFGEC as a Probe to Identify ASCs in Human WAT and Tumors

Paraffin sections of indicated human tissues were incubated with biotinylated CSWKYWFGEC peptide or a scrambled peptide CWWGSFYEKC and subjected to IF with antibodies against CD31 (green) and streptavidin (red). Note that the scrambled peptide does not bind to WAT (B), whereas CSWKYWFGEC-bound cells are observed in s.c. WAT (A) and tumor stroma (D), but not in the lung (C). Nuclei are blue. The scale bar represents 50 μm. Experiments were performed for WAT of three patients with similar results.

progression is driven by these stromal cells[1] that secrete trophic factors[34–36] and mediate the desmoplastic deposition of extracellular matrix (ECM), tumor vascularization, and the epithelial-mesenchymal transition (EMT) enabling metastatic capacity.[37] Tumor stroma also mutes anti-cancer immune response.[38–42] Progression of many types of cancer is promoted by obesity, hallmark of which is WAT overgrowth and high BMI.[2,16,43] The mechanisms underlying increased risk of cancer mortality in obese patients remain unclear. Whereas diet[44] and the metabolic syndrome[45] appear to underlie cancer initiation, different mechanisms account for the effect of obesity on cancer progression. A growing body of evidence indicates that the key determinant of cancer progression in obesity is WAT.[43,46] Consistent with that observation, breast cancer survivors that undergo WAT transplantation for breast augmentation have a higher chance of relapse, as we have reported.[15–17] Factors secreted by ASCs, adipocytes, and infiltrating leukocytes, collectively called adipokines, have been considered as the mechanistic link between obesity and cancer.[47] ASCs also secrete MCP-1 and other chemokines recruiting macrophages[48] that accumulate in the crown-like structures associated with breast cancer risk and progression.[49,50]

At present, there are no therapies aimed at ASCs available due to the lack of validated molecular targets specific for these cells. Previously, we reported non-glycanated ΔDCN as the marker of ASC differentiating into white adipocytes in mice.[29] Here, we demonstrate that human ASC express also non-glycanated DCN recognized by CSWKYWFGEC peptide. We show that this peptide can be used as an imaging probe or a vehicle directing cytotoxic therapeutics to ASCs and enabling their targeted depletion. We had previously reported that, in mice, ngDCN-homing hunter killer peptides D-WAT and D-CAN target PDGFRα-negative/PDGFRβ-positive ASCs serving as progenitors of white adipocytes, whereas they spare the PDGFRα-positive/PDGFRβ-negative brown/beige adipocyte progenitors.[25,29] Our data presented here indicate that both D-WAT and D-CAN also target human ASCs with comparable selectivity. As we had demonstrated in animal studies, ASCs with higher PDGFRα/lower PDGFRβ signaling give rise to beige adipocytes, whereas ASCs with higher PDGFRβ/lower PDGFRα signaling give rise to white adipocytes. It remains to be determined whether ngDCN specifically marks white adipocyte progenitor cells in humans.

Decorin is a ubiquitously expressed proteoglycan secreted into the extracellular matrix molecules. Its main function is modulation of fibrillogenesis through interaction with collagens and fibronectin.[51] Based on the DCN cleavage site resulting in ΔDCN, we have predicted that it is generated post-translationally.[26] The protease generating ΔDCN remains to be identified. Our data showing that ngDCN added to cell culture medium binds to human ASCs (Figure S5) suggest that proteolysis occurs extracellularly. The function of ngDCN remains to be determined. Both DCN and ngDCN have been reported to suppress adipogenesis;[26] however, the mechanism of their effects on specific pre-adipocyte lineages has not been analyzed. It has been shown that DCN suppresses PDGFR signaling by interfering with PDGF activity.[52] In mice, PDGFRα^{-}PDGFRβ^{+} ASCs are perivascular/mural cells, whereas the PDGFRα^{+}PDGFRβ^{-} cells are localized deeper in the stroma.[29] Our data demonstrate that, in human WAT, the two corresponding stromal populations exist and have the same relative perivascular localization. It is possible that DCN and ngDCN regulate adipogenesis by suppressing signaling specifically through PDGFRα or PDGFRβ. The function of DCN and ngDCN interactors, including PDGFs, transforming growth factor β (TGF-β), and resistin, which serves as a ΔDCN receptor in WAT,[26,51] in modulating ASC fate remains to be tested. Studies in mouse models provide evidence that DCN suppresses PDGFRα signaling in liver cancer.[52] Establishing how DCN and ngDCN modulates PDGFRα and PDGFRβ signaling in the context of white and brown adipose tissue, tumors, and other fibrotic conditions may delineate new approaches to disease prevention and treatment.

In summary, this study identifies a cell surface marker through which human ASCs can be identified and depleted. We propose that development of drugs targeting human ASCs can lead to improved combination therapies complementing conventional cancer treatments in cancer patients.

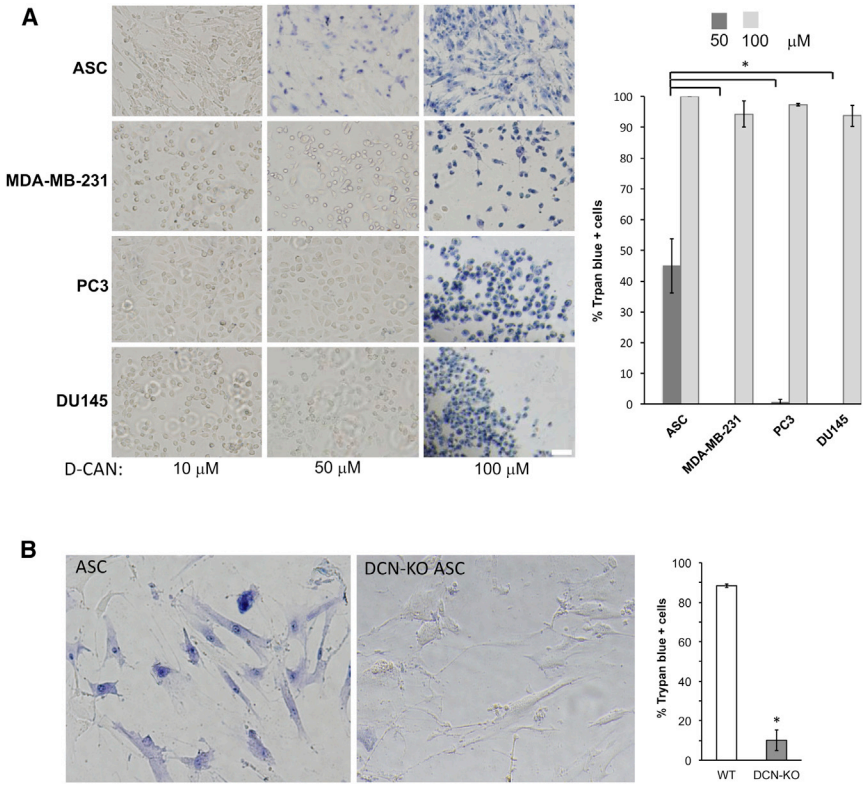

Figure 5. Hunter-Killer Peptide Targeting Human ASCs Expressing DCN

(A) Human subcutaneous ASCs from patient 1, breast adenocarcinoma (MDA-MB-231), and prostate adenocarcinoma (PC3 and DU145) cells were incubated with indicated concentrations of peptide D-CAN. Plotted are mean ± SEM for multiple fields (n = 10). *p < 0.01 (Student's t test). (B) Human unmodified ASCs and DCN-null ASCs (DCN-KO) were incubated with indicated concentrations of peptide D-CAN. After 4 hr treatment, cells were stained with trypan blue. Blue color shows selective killing of ASCs at 0.05 mM. The scale bar represents 50 μm. Plotted are mean ± SEM for multiple fields (n = 10). *p < 0.01 (Student's t test). Experiments were performed for i.p. and s.c. WAT of three patients with similar results.

MATERIALS AND METHODS

Human Subjects

The clinical protocol was approved by the institutional review board (IRB) (protocol HSC-MS-14-0514). For ASC isolation, samples of subcutaneous and omental WAT from three de-identified patients undergoing bariatric surgery (coded as patients 1, 2, and 3) were used with similar results. Paraffin sections analyzed were from WAT of patients 1–3 and from 12 additional patients. Paraffin sections of eight control normal tissues were from human adult multi-tissue panel-I T8234431 (BioChain). Paraffin sections were from the three breast cancer patients (invasive ductal carcinoma [IDC] grade 3 estrogen receptor $[ER]^{+}$progesterone receptor$[PR]^{-}$ stage 3 breast cancer, ductal carcinoma in situ [DCIS] grade 3 $ER^{-}PR^{-}$ stage 0 breast cancer, and IDC grade 2 $ER^{+}PR^{+}$ stage 1 breast cancer) enrolled at MD Anderson Cancer Center and from periprostatic WAT specimens described previously.[2]

Experimental Animals

Animal studies were approved by the Institutional Animal Care and Use Committee of UTHealth. C57BL/6 mice were from Jackson Laboratory. For RM1 tumor cell grafting, 1×10^5 cells were injected with a 21-gauge needle s.c. onto lower back.

Peptides

Proteolysis-resistant WAT7-$KLAKLAK_2$ (D-WAT) and WAT7-$KFAKFAK_2$ (D-CAN) were made as "all-D-amino acid" peptides with the targeting and apoptotic domains linked by aminohexanoic acid linker $NH-(CH_2)_5-CO$. Peptides were synthesized as acetate salt, cysteine cyclized, chromatographically purified to 99%, and quality controlled (mass spectroscopy). D-WAT, CSWKYWFGEC, and $NH-(CH_2)_5$-$KLAKLAK_2$ peptides were purchased from Celtek; D-CAN was purchased from Ambiopharm. Peptides were dissolved in PBS to 10 mM, and aliquots were stored frozen until dilution in PBS, filtration, and use. For peptide administration into mice, the metronomic s.c. injection protocol was used as described,[29] starting the day after tumor grafting. Peptide biotinylation was performed as described.[26] Tissues and live cells were incubated with biotinylated peptides at concentration 10 nM and 20 nM, respectively.

Affinity Chromatography

Protein pull-down assay was performed as described.[26] Cells were disrupted in PBS containing protease inhibitors (PI) cocktail with a Dounce homogenizer; centrifugation (15,000 × *g* for 30 min at 4°C) was performed to separate soluble proteins from membrane pellet. Membrane proteins were solubilized in PBS containing 1 mM $CaCl_2$, 1 mM $MgCl_2$, 50 mM n-octyl-beta-D-glucopyranoside, and PI cocktail (column buffer). Six milligrams of a cysteine-cyclized peptide was coupled onto 250 μL of Affigel 10 (Bio-Rad), and the column was equilibrated with column buffer containing 1% Triton X-100. Peptide-coupled resin (10 μL) was incubated with 30 μg of membrane extract and washed with column buffer. Elution was performed with SDS-PAGE loading buffer. Protein preparations resolved on SDS-PAGE were blotted onto Immobilon-FL membrane (Millipore), blocked with Odyssey blocking buffer (LI-COR Biosciences), and probed (in PBS/0.05% Triton X-100) with 1:1,000 goat anti-DCN (R&D Systems). Signal was detected by Odyssey imaging system using anti-goat IRDye 800CW (LI-COR Biosciences). NS0-expressed murine DCN was from R&D Systems.

Cell Lines and Primary Cell Culture

Cells were cultured in DMEM supplemented with 10% fetal bovine serum (FBS) and penicillin-streptomycin. Cell lines were

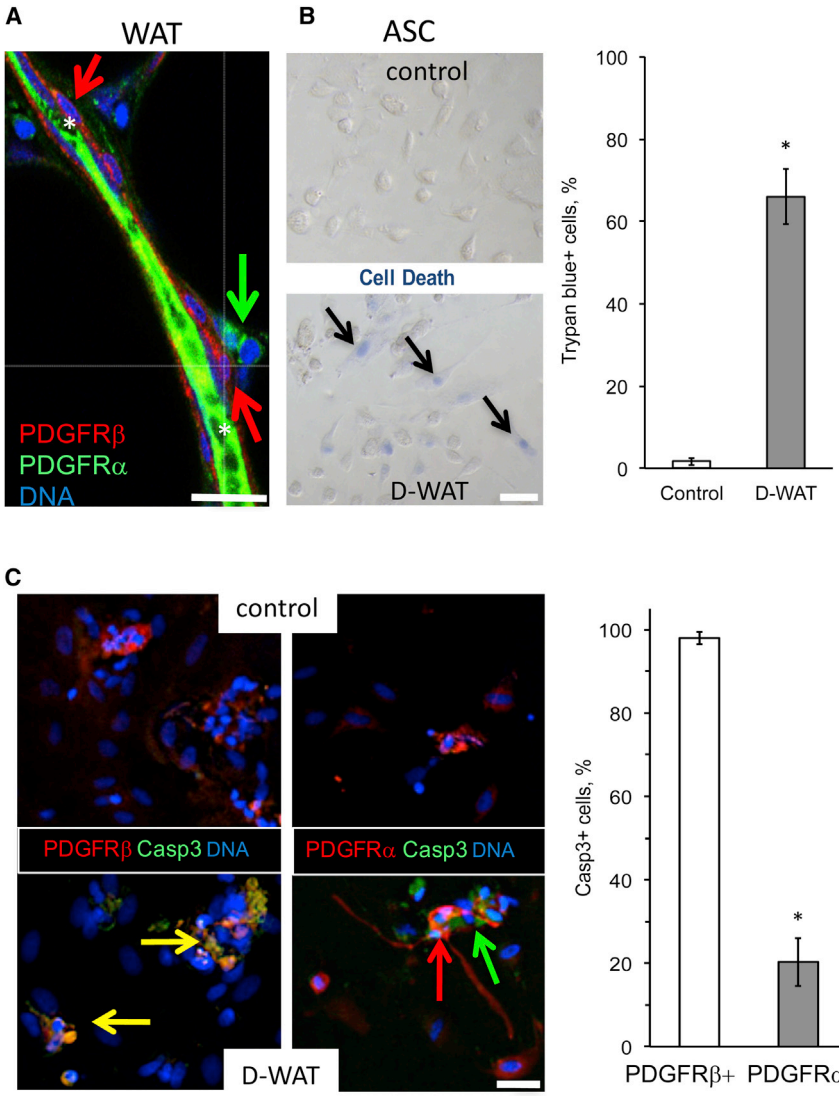

Figure 6. Selective Human PDGFRβ$^+$ ASC Depletion with the Hunter-Killer Peptide

(A) IF of human WAT identifies PDGFRα$^+$PDGFRβ$^-$ and PDGFRα$^-$PDGFRβ+ ASCs as distinct populations located around a blood vessel (*, green autofluorescence). (B) Selective apoptosis of some, but not all, ASCs from human WAT treated with 0.01 mM control peptide or D-WAT is shown. Trypan blue staining (blue) reveals cell death. Plotted are mean ± SEM for multiple fields (n = 10). *p < 0.01 (Student's t test). (C) IF on cells from (B) identifies apoptosis (cleaved caspase 3, green) of PDGFRβ$^+$ cells (yellow), but not of PDGFRα$^+$ cells (red) induced by 0.01 mM D-WAT. The scale bar represents 50 μm. Plotted are mean ± SEM for multiple fields (n = 10). *p < 0.01 (Student's t test). Experiments were performed for i.p. and s.c. WAT of three patients with similar results.

purchased from the American Type Culture Collection. Primary cells were isolated and cultured as described.[5,26] Freshly isolated ASCs were briefly cultured to remove non-adherent cells. Trypan blue exclusion assay was used to determine cell viability in peptide-treated ASCs and tumor cell lines as reported previously.[25,29] When cell density reached 80% confluency, cells were treated with indicated concentrations of peptides in 0.5 mL culture medium for 2 hr. Cells were stained with 0.4% trypan blue solution (MP Biomedicals) for 10 min to visualize live and dead cells. DCN-null ASCs were generated from primary s.c. human ASCs of patient 1 using the CRISPR/Cas9 method.[53] To construct *pLenti-CRISPR/Cas9 hDCN* gRNA expression vectors, the 20-bp target sequence 5′- GGCTCG AAGTCGCGGTCATCAGG-3′ containing the PAM sequence (underlined) was subcloned into *lenti-CRISPR v2* plasmid (Addgene no. 52961).

IF

Sections of formalin-fixed paraffin-embedded tissues were analyzed by IF as described.[5,26] Antigen retrieval, washing with 0.2% Triton X-100, and blocking in Serum-Free Protein Block (Dako) was followed by incubation with primary antibodies (4°C; 12 hr) and secondary antibodies (room temperature [RT]; 1 hr) in PBS containing 0.05% Tween 20. Cells plated on 24-well plate were fixed with 4% paraformaldehyde, permeabilized with Triton X-100, blocked with Serum-Free Protein Block, and followed by incubation with primary and secondary antibodies, as above. Antibodies used were as follows: rabbit anti-mouse PDGFRβ ab32570 (Abcam; 1:100); rabbit anti-CD31 (Santa Cruz Biotechnology; 1:100); goat anti-human PDGFRα (R&D; 1:100); rabbit anti-human PDGFRβ (Abcam; 1:100); and rabbit anti-Asp175-cleaved caspase3 from Cell Signaling Technology (1:100). Alexa-488-conjugated (1:150) and Cy3-conjugated (1:100) streptavidin was from Invitrogen. Secondary antibodies were donkey Alexa-488-conjugated (1:150) immunoglobulin G (IgG) from Invitrogen and Cy3-conjugated (1:300) IgG from Jackson ImmunoResearch. Nuclei were visualized with DAPI. For quantifications, at least ten random 10× or 20× magnification fields were blindly scored and/or measured using microscope grid. Tissue IF images were acquired with Carl Zeiss upright Apotome Axio Imager Z1/ZEN2 Core Imaging software. Cells were imaged using a Leica microscope (Leica Microsystems; model: DM IL LED Fluo).

Statistics

Microsoft Excel was used to graph data as mean ± SEM and to calculate p values using homoscedastic Student's t test.

SUPPLEMENTAL INFORMATION

Supplemental Information includes five figures and can be found with this article online at http://dx.doi.org/10.1016/j.omto.2017.05.003.

AUTHOR CONTRIBUTIONS

M.G.K. designed the experiments, analyzed data, and wrote the manuscript; A.C.D. designed and conducted the experiments and analyzed data; A.D. conducted the experiments; and B.S., X.W., A.A.S., and N.T.U. provided materials, analyzed data, and edited the manuscript.

CONFLICTS OF INTEREST

The authors declare no conflict of interest.

ACKNOWLEDGMENTS

We thank Zhanguo Gao and Angielyn Rivera for technical assistance. We thank Renato Iozzo and Jane Grande-Allen for sharing DCN-null MEFs. We thank Askar Kuchumov, Eugene Shevchenko, and Andrew Makarovskiy for many helpful discussions. This work was supported in part by CTSA award UL1 TR000371.

REFERENCES

1. Kolonin, M.G., Evans, K.W., Mani, S.A., and Gomer, R.H. (2012). Alternative origins of stroma in normal organs and disease. Stem Cell Res. (Amst.) *8*, 312–323.
2. Zhang, T., Tseng, C., Zhang, Y., Sirin, O., Corn, P.G., Li-Ning-Tapia, E.M., Troncoso, P., Davis, J., Pettaway, C., Ward, J., et al. (2016). CXCL1 mediates obesity-associated adipose stromal cell trafficking and function in the tumour microenvironment. Nat. Commun. *7*, 11674–11690.
3. Zhang, Y., Daquinag, A., Traktuev, D.O., Amaya-Manzanares, F., Simmons, P.J., March, K.L., Pasqualini, R., Arap, W., and Kolonin, M.G. (2009). White adipose tissue cells are recruited by experimental tumors and promote cancer progression in mouse models. Cancer Res. *69*, 5259–5266.
4. Klopp, A.H., Zhang, Y., Solley, T., Amaya-Manzanares, F., Marini, F., Andreeff, M., Debeb, B., Woodward, W., Schmandt, R., Broaddus, R., et al. (2012). Omental adipose tissue-derived stromal cells promote vascularization and growth of endometrial tumors. Clin. Cancer Res. *18*, 771–782.
5. Zhang, Y., Daquinag, A.C., Amaya-Manzanares, F., Sirin, O., Tseng, C., and Kolonin, M.G. (2012). Stromal progenitor cells from endogenous adipose tissue contribute to pericytes and adipocytes that populate the tumor microenvironment. Cancer Res. *72*, 5198–5208.
6. Kolonin, M.G., and Simmons, P.J. (2009). Combinatorial stem cell mobilization. Nat. Biotechnol. *27*, 252–253.
7. Zhang, Y., Bellows, C.F., and Kolonin, M.G. (2010). Adipose tissue-derived progenitor cells and cancer. World J. Stem Cells *2*, 103–113.
8. Bellows, C.F., Zhang, Y., Chen, J., Frazier, M.L., and Kolonin, M.G. (2011). Circulation of progenitor cells in obese and lean colorectal cancer patients. Cancer Epidemiol. Biomarkers Prev. *20*, 2461–2468.
9. Bellows, C.F., Zhang, Y., Simmons, P.J., Khalsa, A.S., and Kolonin, M.G. (2011). Influence of BMI on level of circulating progenitor cells. Obesity (Silver Spring) *19*, 1722–1726.
10. Kidd, S., Spaeth, E., Watson, K., Burks, J., Lu, H., Klopp, A., Andreeff, M., and Marini, F.C. (2012). Origins of the tumor microenvironment: quantitative assessment of adipose-derived and bone marrow-derived stroma. PLoS ONE *7*, e30563.
11. Martin-Padura, I., Gregato, G., Marighetti, P., Mancuso, P., Calleri, A., Corsini, C., Pruneri, G., Manzotti, M., Lohsiriwat, V., Rietjens, M., et al. (2012). The white adipose tissue used in lipotransfer procedures is a rich reservoir of CD34+ progenitors able to promote cancer progression. Cancer Res. *72*, 325–334.
12. Lin, G., Yang, R., Banie, L., Wang, G., Ning, H., Li, L.C., Lue, T.F., and Lin, C.S. (2010). Effects of transplantation of adipose tissue-derived stem cells on prostate tumor. Prostate *70*, 1066–1073.
13. Orecchioni, S., Gregato, G., Martin-Padura, I., Reggiani, F., Braidotti, P., Mancuso, P., Calleri, A., Quarna, J., Marighetti, P., Aldeni, C., et al. (2013). Complementary populations of human adipose CD34+ progenitor cells promote growth, angiogenesis, and metastasis of breast cancer. Cancer Res. *73*, 5880–5891.
14. Rowan, B.G., Gimble, J.M., Sheng, M., Anbalagan, M., Jones, R.K., Frazier, T.P., Asher, M., Lacayo, E.A., Friedlander, P.L., Kutner, R., and Chiu, E.S. (2014). Human adipose tissue-derived stromal/stem cells promote migration and early metastasis of triple negative breast cancer xenografts. PLoS ONE *9*, e89595.
15. Bertolini, F., Petit, J.Y., and Kolonin, M.G. (2015). Stem cells from adipose tissue and breast cancer: hype, risks and hope. Br. J. Cancer *112*, 419–423.
16. Bertolini, F., Orecchioni, S., Petit, J.Y., and Kolonin, M.G. (2014). Obesity, proinflammatory mediators, adipose tissue progenitors, and breast cancer. Curr. Opin. Oncol. *26*, 545–550.
17. Bertolini, F., Lohsiriwat, V., Petit, J.Y., and Kolonin, M.G. (2012). Adipose tissue cells, lipotransfer and cancer: a challenge for scientists, oncologists and surgeons. Biochim. Biophys. Acta *1826*, 209–214.
18. Nowicka, A., Marini, F.C., Solley, T.N., Elizondo, P.B., Zhang, Y., Sharp, H.J., Broaddus, R., Kolonin, M., Mok, S.C., Thompson, M.S., et al. (2013). Human omental-derived adipose stem cells increase ovarian cancer proliferation, migration, and chemoresistance. PLoS ONE *8*, e81859.
19. Salimian Rizi, B., Caneba, C., Nowicka, A., Nabiyar, A.W., Liu, X., Chen, K., Klopp, A., and Nagrath, D. (2015). Nitric oxide mediates metabolic coupling of omentum-derived adipose stroma to ovarian and endometrial cancer cells. Cancer Res. *75*, 456–471.
20. Rodeheffer, M.S., Birsoy, K., and Friedman, J.M. (2008). Identification of white adipocyte progenitor cells in vivo. Cell *135*, 240–249.
21. Traktuev, D.O., Merfeld-Clauss, S., Li, J., Kolonin, M., Arap, W., Pasqualini, R., Johnstone, B.H., and March, K.L. (2008). A population of multipotent CD34-positive adipose stromal cells share pericyte and mesenchymal surface markers, reside in a periendothelial location, and stabilize endothelial networks. Circ. Res. *102*, 77–85.
22. Berry, R., and Rodeheffer, M.S. (2013). Characterization of the adipocyte cellular lineage in vivo. Nat. Cell Biol. *15*, 302–308.
23. Lee, Y.H., Petkova, A.P., Mottillo, E.P., and Granneman, J.G. (2012). In vivo identification of bipotential adipocyte progenitors recruited by β3-adrenoceptor activation and high-fat feeding. Cell Metab. *15*, 480–491.
24. Tang, W., Zeve, D., Suh, J.M., Bosnakovski, D., Kyba, M., Hammer, R.E., Tallquist, M.D., and Graff, J.M. (2008). White fat progenitor cells reside in the adipose vasculature. Science *322*, 583–586.
25. Daquinag, A.C., Tseng, C., Zhang, Y., Amaya-Manzanares, F., Florez, F., Dadbin, A., Zhang, T., and Kolonin, M.G. (2016). Targeted proapoptotic peptides depleting adipose stromal cells inhibit tumor growth. Mol. Ther. *24*, 34–40.
26. Daquinag, A.C., Zhang, Y., Amaya-Manzanares, F., Simmons, P.J., and Kolonin, M.G. (2011). An isoform of decorin is a resistin receptor on the surface of adipose progenitor cells. Cell Stem Cell *9*, 74–86.
27. Kolonin, M.G., Saha, P.K., Chan, L., Pasqualini, R., and Arap, W. (2004). Reversal of obesity by targeted ablation of adipose tissue. Nat. Med. *10*, 625–632.
28. Chorev, M., and Goodman, M. (1995). Recent developments in retro peptides and proteins–an ongoing topochemical exploration. Trends Biotechnol. *13*, 438–445.
29. Daquinag, A.C., Tseng, C., Salameh, A., Zhang, Y., Amaya-Manzanares, F., Dadbin, A., Florez, F., Xu, Y., Tong, Q., and Kolonin, M.G. (2015). Depletion of white adipocyte progenitors induces beige adipocyte differentiation and suppresses obesity development. Cell Death Differ. *22*, 351–363.
30. Ferdous, Z., Peterson, S.B., Tseng, H., Anderson, D.K., Iozzo, R.V., and Grande-Allen, K.J. (2010). A role for decorin in controlling proliferation, adhesion, and migration of murine embryonic fibroblasts. J. Biomed. Mater. Res. A *93*, 419–428.
31. Nie, J., Chang, B., Traktuev, D.O., Sun, J., March, K., Chan, L., Sage, E.H., Pasqualini, R., Arap, W., and Kolonin, M.G. (2008). IFATS collection: Combinatorial peptides identify α5β1 integrin as a receptor for the matricellular protein SPARC on adipose stromal cells. Stem Cells *26*, 2735–2745.

32. Azhdarinia, A., Daquinag, A.C., Tseng, C., Ghosh, S.C., Ghosh, P., Amaya-Manzanares, F., Sevick-Muraca, E., and Kolonin, M.G. (2013). A peptide probe for targeted brown adipose tissue imaging. Nat. Commun. *4*, 2472–2482.

33. Hanahan, D., and Coussens, L.M. (2012). Accessories to the crime: functions of cells recruited to the tumor microenvironment. Cancer Cell *21*, 309–322.

34. Fukumura, D., Xavier, R., Sugiura, T., Chen, Y., Park, E.C., Lu, N., Selig, M., Nielsen, G., Taksir, T., Jain, R.K., and Seed, B. (1998). Tumor induction of VEGF promoter activity in stromal cells. Cell *94*, 715–725.

35. Bissell, M.J., and Radisky, D. (2001). Putting tumours in context. Nat. Rev. Cancer *1*, 46–54.

36. Coussens, L.M., and Werb, Z. (2002). Inflammation and cancer. Nature *420*, 860–867.

37. Kalluri, R., and Zeisberg, M. (2006). Fibroblasts in cancer. Nat. Rev. Cancer *6*, 392–401.

38. Shojaei, F., Zhong, C., Wu, X., Yu, L., and Ferrara, N. (2008). Role of myeloid cells in tumor angiogenesis and growth. Trends Cell Biol. *18*, 372–378.

39. Bertolini, F., Shaked, Y., Mancuso, P., and Kerbel, R.S. (2006). The multifaceted circulating endothelial cell in cancer: towards marker and target identification. Nat. Rev. Cancer *6*, 835–845.

40. Wels, J., Kaplan, R.N., Rafii, S., and Lyden, D. (2008). Migratory neighbors and distant invaders: tumor-associated niche cells. Genes Dev. *22*, 559–574.

41. Dvorak, H.F. (1986). Tumors: wounds that do not heal. Similarities between tumor stroma generation and wound healing. N. Engl. J. Med. *315*, 1650–1659.

42. Lu, P., Weaver, V.M., and Werb, Z. (2012). The extracellular matrix: a dynamic niche in cancer progression. J. Cell Biol. *196*, 395–406.

43. Sirin, O., and Kolonin, M.G. (2013). Treatment of obesity as a potential complementary approach to cancer therapy. Drug Discov. Today *18*, 567–573.

44. Hursting, S.D., Lavigne, J.A., Berrigan, D., Perkins, S.N., and Barrett, J.C. (2003). Calorie restriction, aging, and cancer prevention: mechanisms of action and applicability to humans. Annu. Rev. Med. *54*, 131–152.

45. Cowey, S., and Hardy, R.W. (2006). The metabolic syndrome: a high-risk state for cancer? Am. J. Pathol. *169*, 1505–1522.

46. Park, J., Morley, T.S., Kim, M., Clegg, D.J., and Scherer, P.E. (2014). Obesity and cancer–mechanisms underlying tumour progression and recurrence. Nat. Rev. Endocrinol. *10*, 455–465.

47. Park, J., Euhus, D.M., and Scherer, P.E. (2011). Paracrine and endocrine effects of adipose tissue on cancer development and progression. Endocr. Rev. *32*, 550–570.

48. Murdoch, C., Muthana, M., Coffelt, S.B., and Lewis, C.E. (2008). The role of myeloid cells in the promotion of tumour angiogenesis. Nat. Rev. Cancer *8*, 618–631.

49. Iyengar, N.M., Brown, K.A., Zhou, X.K., Gucalp, A., Subbaramaiah, K., Giri, D.D., Zahid, H., Bhardwaj, P., Wendel, N.K., Falcone, D.J., et al. (2017). Metabolic obesity, adipose inflammation and elevated breast aromatase in women with normal body mass index. Cancer Prev. Res. (Phila.) *10*, 235–243.

50. Mullooly, M., Yang, H.P., Falk, R.T., Nyante, S.J., Cora, R., Pfeiffer, R.M., Radisky, D.C., Visscher, D.W., Hartmann, L.C., Carter, J.M., et al. (2017). Relationship between crown-like structures and sex-steroid hormones in breast adipose tissue and serum among postmenopausal breast cancer patients. Breast Cancer Res. *19*, 8.

51. Gubbiotti, M.A., Vallet, S.D., Ricard-Blum, S., and Iozzo, R.V. (2016). Decorin interacting network: a comprehensive analysis of decorin-binding partners and their versatile functions. Matrix Biol. *55*, 7–21.

52. Baghy, K., Horváth, Z., Regős, E., Kiss, K., Schaff, Z., Iozzo, R.V., and Kovalszky, I. (2013). Decorin interferes with platelet-derived growth factor receptor signaling in experimental hepatocarcinogenesis. FEBS J. *280*, 2150–2164.

53. Cong, L., Ran, F.A., Cox, D., Lin, S., Barretto, R., Habib, N., Hsu, P.D., Wu, X., Jiang, W., Marraffini, L.A., and Zhang, F. (2013). Multiplex genome engineering using CRISPR/Cas systems. Science *339*, 819–823.